

DESIGN OF A LOW-POWER AND HIGH THROUGHPUT ERROR DETECTION AND CORRECTION CIRCUIT USING THE 4T EX-OR METHOD

S. KAVITHA*, FAZIDA HANIM HASHIM, MD MAMUN IBNE REAZ,
NOORFAZILA KAMAL

Department of Electrical, Electronic and Systems Engineering, Universiti Kebangsaan
Malaysia, 43600, UKM, Bangi, Selangor, Malaysia

*Corresponding Author: kavithapari@gmail.com

Abstract

This paper describes an efficient implementation of an error correction circuit based on single error detection and correction with check bit pre-computation. The core component of the proposed 4-bit EX-OR circuit was designed using the CMOS cascade method. This paper presents a 4-input EX-OR gate that was developed from a 2-input EX-OR gate using the bit slice method. The proposed architecture retains the modified Error Correction Code (ECC) circuit. The proposed 4-input EX-OR gate and its auxiliary components such as AND, MUX and D Flip-Flop were schematized using the DSCH tool and the layouts was analysed using the BSIM4 analyser. The simulation results were obtained and compared with the performance of existing circuits. LVS verification was performed on the modified ECC circuit at CMOS 70 nm feature size and its corresponding voltage of 0.7V. The modified ECC circuit simulation results were analysed and compared with the performance of existing circuits in terms of propagation delay, power dissipation, area, latency, and throughput. The proposed ECC circuit showed an improved performance with existing circuit low power dissipation (94.41%) and high throughput (95.20%).

Keywords: EX-OR gate, ECC, MUX, Power dissipation, Propagation delay, Throughput, BSIM 4.

1. Introduction

The detection of unexpected information forms the basis of all error detection and correction in hard disks. In order to get useful information, additional bits are added to each sector of a hard disk for the purpose of error detection and correction [1]. These additional bits, called the error correction code, are

Nomenclatures

C_{gol}	Gate to Diffusion Overlap Capacitance
C_{jb}	Junction biasing Capacitance
C_{jbsw}	Junction Side Wall Capacitance
C_{out}	Output Capacitance
R_n	NMOS resistive
R_p	PMOS resistive

Greek Symbols

τ_n	Propagation delay time of NMOS transistor
τ_p	Propagation delay time of PMOS transistor.

Abbreviations

BSIM	Berkeley Spice Simulator
DED	Double Error Detection
DSCH	Digital Schematic
ECC	Error Correction Circuit
EDAC	Error Detection And Correction
EPI	Energy Per Instruction
LDPC	Low Density Parity Check
LVS	Layout Versus Simulation
MUX	Multiplexer
PERR	Parity Error
PGEN	Parity Generation
PTL	Pass Transistor Logic
SEC	Single Error Correction
SED	Single Error Detection
VTC	Voltage Transfer Characteristic

introduced into the hardware through the error correcting circuit [2]. These bits contain information that can be used to correct errors found while trying to access the data bits [3]. When a sector is written on a disk, the Error Correcting Code (ECC) codes are generated and stored in the reserved bits. During the read operation, the data that was fetched from the sector are combined with the ECC bits and sent to the controller. At this point any errors will be detected and conveyed to the system. This data stream will then be corrected by the controller before the data can be passed through to the rest of the system [4]. In addition, the system will also keep track of damaged data including all errors detected during the event. Most modern day hardware contains an advanced firmware that uses ECC as part of its overall error management protocol.

The parity bit is simple method of error detection mechanism, which is commonly used to detect an odd-numbered errors [5]. In parity bit operation, the data bits are broken up into blocks of bits and the total number of bits with the value 1 is counted. The parity bit is then set based on whether the value is odd or even before it is added to the end of the string of bits [6].

At the receiving end, the blocks of bits are tested to verify that there is no error in the data by recalculating the number of bits with the value of 1 and comparing it with the parity bit value. However, parity bit can only detect corruption in the data if the number of errors appearing in the string of bits is odd, whereas strings with even number of errors will be mistaken as being correct [7]. In short, a parity bit can only perform Single Error Detection (SED) which can only detect a string of bits with odd number of errors.

In order to address this shortcoming, various approaches have been proposed such as Double Error Detection (DED) and Single Error Correction (SEC), or more commonly known as SEC/DED schemes [8]. These SEC/DED schemes are based on either the Hamming code or the LDPC code. This paper deals with correction code using the SED method for ECC. A 4-bit EX-OR gate is proposed as the core component of the ECC circuit. It computes Hamming values into parity bits via a proposed EX-OR circuit. The proposed 2 input EX-OR circuit is designed using CMOS. Whereas previous research work has focused on minimizing area and delay in ECC circuit, this paper focuses mainly on minimizing power, improving speed and throughput, and reducing the chip area. By taking power into consideration during the design of the modified ECC circuit, significant reductions in power usage was achieved. The rest of the paper is organized as follows: Section 2 presents the related works and underlying prompt behind our design, Section 3 describes the design method, Section 4 presents our results and discussions (simulation results & parity analysis of EX-OR 4T based ECC circuit and comparison of the performance with hardening strategies), and Section 5 concludes the paper and suggests further studies in the future.

2. Related works

Stefano et al. [7] proposed an ECC circuit using NAND flash memory, which has inspired the design of our own circuit. Research on the improvement of error correction strategies using NAND flash memory needs to be done to further improve on its performance and dependability. Stefano et al. proposed a circuit that integrates error correction together with detection, which results in a fault-tolerant mass-memory device. So far, no systematic approach has been proposed to take the system as a whole into consideration. Stefano et al. established that being a combinational gate design, NAND flash memory design gives a better performance compared to other designs from earlier research.

Whatmough et al. [9] presented a 1GHz Razor FIR accelerator in CMOS 70nm process. The Razor latches were positioned at critical paths for the purpose of implementing timing error detection. The combination of two distinct mechanisms achieved fixed latency error correction in real time DSP systems. Whatmough et al. [9] proposed that time-borrow tracking algorithm is used for timing-error detection to track excessive time borrowing and correct marginal timing violations. At the end of the pipeline, persistent unresolved time borrowing can be corrected within the pipeline using a low-overhead approximate error-correction stage which is based on interpolation. The Razor FIR accelerator circuit consists of complex nodes that give higher power dissipation and low speed. These proposals were taken into consideration in our proposed design.

Kun Ma et al. [10] proposed a high performance error detection and fault correction scheme. The proposed circuit maintains the efficiency of low cost implementation by using Montgomery ladder algorithm while showing good performance against both environmental-induced faults as well as attacker-introduced faults. The proposed error detection and correction system achieved better performance in terms of power dissipation and speed than competing circuits. However, circuit analysis of the architecture proposed by Kun Ma et al. shows high power usage at the input and output compared with other error detection and correction architectures. These drawbacks were addressed in our proposed design.

Daniel Gomez Toro et al. [11] proposed a low density soft error correction in memory circuits with high integration and lower power technologies. The proposed system not only deals with memories and latches, but also combinatorial circuits. Hardening by design technique, which is accomplished by increasing the amount of charge representing the bit has been commonly used over the years. The author proposes a system that acts as a single-event transient (SET) filter and as a checkpoint with self-healing properties against top event SET propagation. This is achieved through the use of feedback from bulk built-in current sensors. Our proposed EX-OR circuit rectifies all the errors mentioned above by having a regular arrangement of the transistor.

3. Design method

Several ECC techniques are being used to enhance memory reliability. Among these, the extended Hamming and odd-weight column codes, which fall into the single error correction and double error detection (SEC/DED) code category, are commonly used. These codes consist of two fields; the data or information field and the check bit or parity bit field. Hamming code is a weight-based code, where each position of bit is assigned a weight. The data bits are assigned non power of two weights while the check bits are assigned power of two weights. Error coverage for a unique subset of information bits is provided by each parity bit. This information bits is called a parity group [12, 13]. The basis of our work involves applying the idea of error detection and correction code and improving this technique for improved performance. The design idea of the ECC circuit is shown in Fig. 1.

The proposed ECC circuit uses many components such as EX-OR, AND, MUX and D Flip-Flop circuit. All the above-mentioned combinational circuits are designed using the Pass Transistor Logic (PTL) concept. The proposed 4-bit EX-OR gate, the core component of the proposed ECC circuit, was designed using the dynamic logic technique and consists of 12 transistors. Existing 3T EX-OR and PTL based EX-OR circuits are used as the benchmark for the purpose of evaluating the performance of our proposed circuit. The proposed 4-input EX-OR logic gate is designed based on the push-pull configuration method of CMOS architecture, which involves the use of voltage controlled circuits. The input performance is based on the PMOS and NMOS characteristics [14]. If input is *logic '0'*, both the output and input terminal voltage will be equal to zero. This state, called the *OFF* state, can initiate the push-pull of the EX-OR gate. For an EX-OR circuit, having input $A = 0$ and $B = 0$ will result in output being '*0*'. In the circuit realization, input A goes to the first PMOS source input and second CMOS

gate input. Simultaneously, input B goes to N_2 transistor and input A also goes to N_1 transistor. Using this configuration, the output may logically be zero. When input $A = 1$, and $B = 0$, P_1 transistor gets activated and gives a logic '1' in the output node. During NMOS operation when $B = 0$ and $A = 1$, N_2 transistor is inactive and N_1 transistor gets activated, and pulls the output to logic '1'. This circuit is behaving in a push-pull configuration, therefore resulting in no output losses or charge losses in the output node due to the CMOS technique used. The above-mentioned method will lead to lower power dissipation in the output node. The EX-OR and EX-NOR truth tables is the origin of the mirror circuits. These circuits have 2 inputs which is assigned as A and B . Each given output based on high (V_{DD}) and low ($0V$). This involves two paths from the output to ground, and two paths from the output to the power supply. Each path holds two serially connected FETs.

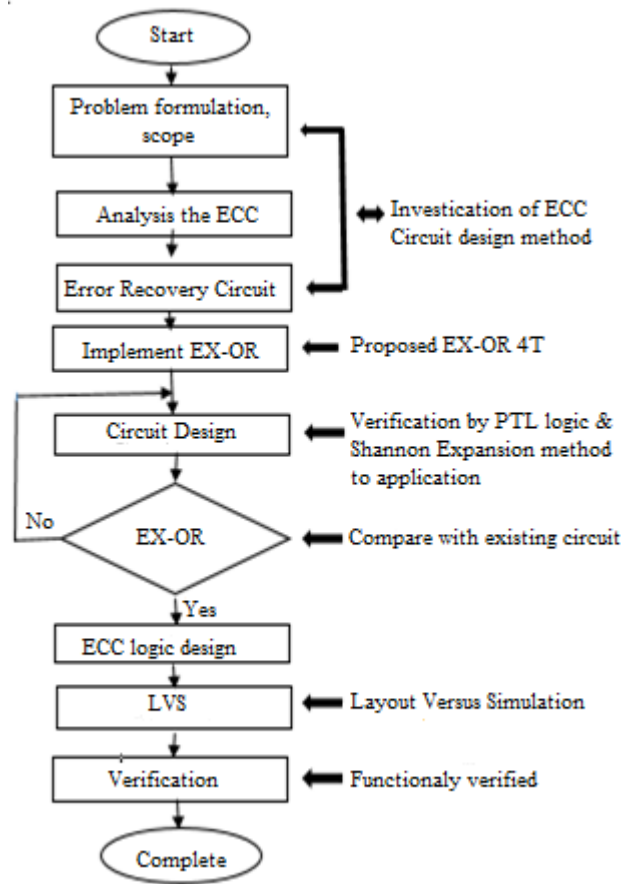


Fig. 1. Design flow diagram.

The EX-OR circuit provides two different combination logics. The current charges follow a combination of two paths and connections should be provided from the output to ground and from the output to the power supply. A proposed 4

input EX-OR circuit is designed using the abovementioned method, which is shown in Fig. 2.

If there is mirror effect at the output node, the design would appear as a reflection of other half of the gate. It can then be said that these functions do not have series in parallel structuring.

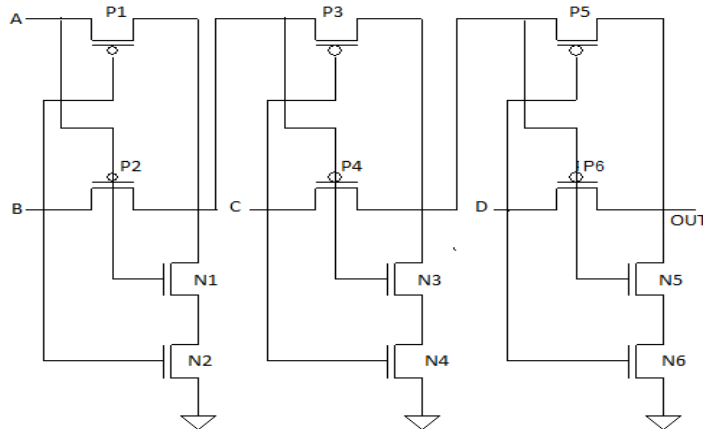


Fig. 2. Proposed 4-bit EX-OR circuit.

The 4 bit EX-OR circuit is designed using 6 PMOS transistors and 3 NMOS transistor as shown in Fig. 3. The PMOS and NMOS transistors work as pass transistors which means that there is no power grid voltages. Since there are no forces of electron flow, this circuit dominates electron transportation as a whole. This EX-OR circuit does not exhibit equal transport phenomena, thus resulting in high power dissipation and delays. The EX-OR 3T circuit gives imbalanced node which gives huge power dissipations. The 6T EX-OR gate gives skew problem due to excessive usage of inverters. Therefore, the proposed EX-OR 4T circuit minimizes the above mentioned problem and provide better performance than the EX-OR 3T and EX-OR 6T circuits.

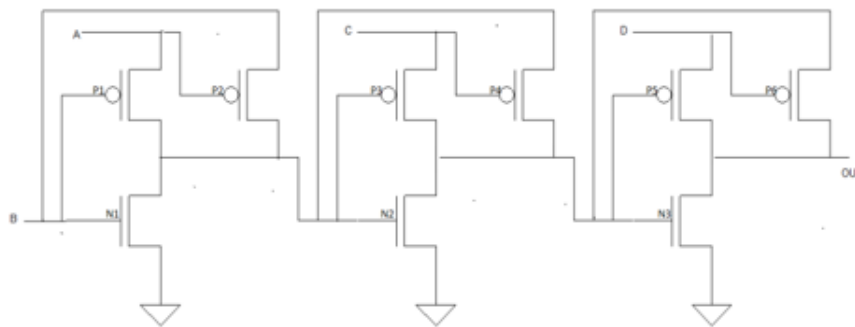


Fig. 3. 4-bit EX-OR circuit (3T model).

The 4-bit EX-OR circuit is designed using pass transistor logic using 12 NMOS transistors and 6 PMOS transistors as shown in Fig. 4. The 2 input MUX circuit is designed with 6 transistors using Pass Transistor Logic (PTL) which will give smooth output voltage curve at the output node. The pass transistor has many gate switches in terms of inverters. The inverters deliver power for supplying the gate to source capacitance. Due to the usage of many inverters which dissipate more power through C_{gs} , this circuit is affected by the skew problem. This skew problem results in high power dissipation and delay in the circuit.

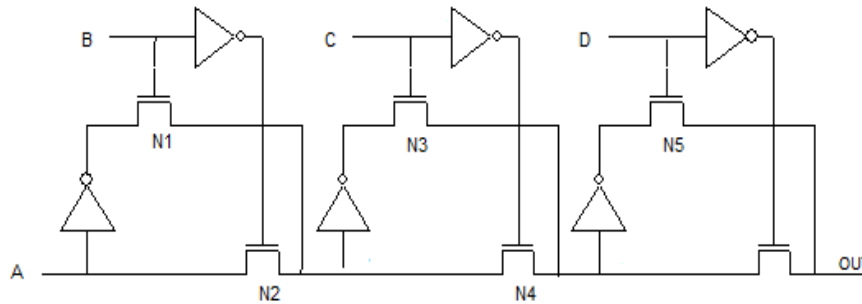


Fig. 4. 4-bit EX-OR circuit (6T PTL model).

3.1. ECC characteristics

Normally the ECC circuits have an error in a digital signal, which occurs from induced voltage noise or other impairments during the transmission of the digital signal from the transmitter to the receiver. During data transmission, extra data bits are added to a message for the purpose of redundancy check. Error detection codes are transmitted as additional data bits appended to the original data bits [15]. Our proposed ECC circuit trades off the abovementioned error. The data input values are checked to verify its accuracy, and an unexpected outcome assumed as an error will be corrected before the signal can be accepted.

The Error detection and correction circuits is most commonly realized using a suitable hash function. A hash function adds a 32 bit IEEE format fixed-length *tag* to a binary digit message, which enables the receiver/transmitter to verify the delivered message using a benchmark algorithm with the tag and comparing it with the one provided. There are many different error correction codes in existence [15]. The reason for the different codes being used in different applications has to do with historical development of the data storage, the types of data errors occurring and the overhead associated with each of the error detection techniques.

3.2. Modified ECC circuit

According to literature review the existing ECC circuit has high power dissipation, higher delay in propagating signal and low throughput. The modified ECC circuit designs are to improve trade off existing circuits. The existing error

correction and detection circuits are used in asynchronous signal for D Flip-Flop. The asynchronous signal may produce higher delay in circuit due to large amount of transistors. The modified ECC circuit (Fig. 5) is implemented using the proposed EX-OR and its auxiliary circuit, which used fewer number of transistor. The modified ECC circuit can be used for Hamming code design principles for its simplicity. Hamming code is used to detect and correct the error in either the check bits or redundant bits generated from the data. This code provides better and more secured data transmission in noisy environment. Moreover, the proposed method can be used with any memory word size.

The modified ECC circuit structure utilise the basic components such as EX-OR, MUX, and D Flip-Flop that are implemented into ECC architecture. This ECC circuits get computational binary input from the bit patterns. The code word structure mainly contains two fields such as data field and check field. These code words are arranged into 12 bits word whereas data bits contain 8 bits and check bits contain 4 bits. According to the Hamming code, the check bits will calculate and investigate the error bit. The error code may be generated by given input data bits pattern. The generated error bit is checked in parity checker circuit. The ECC circuit mainly has 3 outputs which is P5, Parity Generation (PGEN) and Parity Error (PERR). The generated parity word is then delivered in output P5. Depending on the data input, the parity generation is checked with another evaluation code (reference code). PGEN is gated with the BPAR input and it provides word parity after Odd/Even parity control. PGEN also feeds into a 1-bit shift register. The data errors are analysed using parity generation code with enabled input checker. If the parity generates ODD parity, the MUX circuit will generate logic high and vice versa.

The ECC circuit is dependent on the error bit position. The generated bits are used to correct the error bit by applying suitable parity bit. The MUX2 circuit and D Flip-Flop circuit are combined together to perform correction on the error bit. The ECC modules and EX-OR 4-bit module perform a sequence of operations and store the values in the D Flip-Flop register. The errors in the data path will lead to erroneous values which will then be stored in the register and occur in the data path. This causes ON/OFF and set to correct the value that would have been stored in the register. If a D Flip-Flop is used as a register it will cause errors in the data path (D register at different time may affect different operation). This can be corrected using a 4-bit syndrome in EX-OR gate. Similarly, the 8-bit words are corrected if it has the error bit. This modified ECC circuit is schematized using the DSCHEM and layouts are analysed using the BSIM4 analyser.

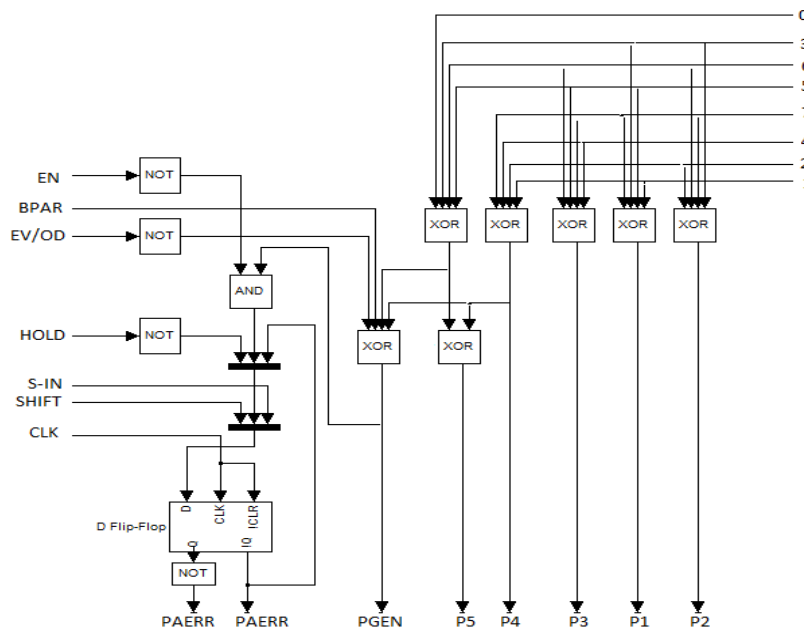


Fig. 5. Modified ECC circuit.

4. Results and Discussion

In order to analyse the behaviour of the ECC, its layout was first schematized using the DSCH tool. Simulation was then performed using the Microwind tool and parametric analyses were done using the BSIM4 analyser. The layouts were analysed at different feature sizes, namely CMOS 180nm, 120nm, 90nm, and 70nm at its corresponding output voltages of 2V, 1.2V, 1V, and 0.7V, respectively. The LVS was done to analyse the power dissipation, delay, and area measurements. The BSIM 4 was used to perform the interconnect analyses of the ECC circuit.

For the purpose of comparison and benchmarking, we compared the performance of our proposed 4 bit EX-OR 4T circuit against those of the 4 bit EX-OR 3T and 4 bit EX-OR 6T circuits. The simulation results of the proposed 4 bit EX-OR 4T and the 4 bit EX-OR 3T and 4 bit EX-OR 6T circuits are shown in Table 1. Our proposed EX-OR 4T gate results in power dissipation of lower than 100 nanowatts, and delay in the low pico seconds, due to the dynamic CMOS logic design and push-pull configuration method. This method can be used to reduce the number of transistors without resulting in any change in the original EX-OR characteristic. The transistor used in the circuit reduced the critical path due to dynamic range, resulting in low power dissipation in the EX-OR circuit. On the other hand, the EX-OR 3T transistor circuit resulted in higher power dissipation than our proposed circuit due to unequal transistor tree, which requires higher logical effort. This effort will lead to power dissipation in the lower level transistor tree structure. Even though the number of transistors is reduced, the power dissipation and delay increased drastically due to the unequal tree structure. As for the EX-OR 6T circuit, the presence of an inverter circuit in its

design creates skewing problem, which results in high power dissipation in the output node.

The power dissipation of the proposed 4 bit EX-OR 4T gate is an order of magnitude lower than the other circuits due to the push-pull configuration design method. In accordance with VLSI design concepts, the use of EX-OR may increase the delay due to switching activity, but our proposed circuits replace switching activities with pull-up and pull-down network of dynamic CMOS technology. So the delay also decreased, so much so as performing even better than the other circuits.

Table 1. Simulation results of 4-bit EX-OR gate and compared with 4 bit EX-OR 3T, 4 bit EX-OR 6T in terms of propagation delay, power dissipation, prea, throughput, latency and EPI.

Circuit	size (nm)	Power $\times 10^{-09}$	Delay (ps)	Area (μm^2)	L (T) ns	R Gbps	EPI(j/s) $\times 10^{-12}$
EX-OR4T	70	17.8	2	176	2.01	1.990	17.874
	90	19.2	6	300	2.009	2.044	38.792
	120	84.4	5	336	1.954	2.047	57.136
	180	55.4	19	897	2.128	2.011	183.205
EX-OR3T	70	699	23	96	2.094	1.910	15.504
	90	701	9	120	2.055	1.946	37.614
	120	7060	9	180	2.071	1.931	61.112
	180	7030	41	660	2.199	1.819	182.458
EX-OR6T	70	287	20	117	2.099	1.905	15.158
	90	8573	18	140	1.956	1.991	12.621
	120	2805	29	192	2.05	1.951	28.066
	180	66320	22	792	1.989	1.879	65.394

L = Latency, R= Throughput

The 4 bit EX-OR 4T circuit was compared with the EX-OR 3T and EX-OR 6T circuits in terms of power dissipation, delay, area, latency, throughput and EPI for feature size 70nm and its corresponding voltage of 0.7V. In terms of power dissipation, the EX-OR 4T performed 97.45% and 93.79% better compared with EX-OR 3T and EX-OR 6T circuits, respectively. The balanced PMOS and NMOS transistor tree structure gives an equal amount of sharing charges to the output transistor. In terms of delay, the proposed EX-OR 4T managed to improve upon the EX-OR 3T and EX-OR 6T by 91.3% and 90%, respectively. This is due to the fact that the times for the transition of rise and fall are equal. When comparison is made in terms of area, the proposed EX-OR 4T compared with EX-OR 3T and EX-OR 6T has improved our circuit 45% and 33% respectively due to number of transistor reduced in the design approach. Looking at latency, the proposed EX-OR 4T circuit compared favourably with the EX-OR 3T and EX-OR 6T by 4% and 4.2%, respectively. Similarly, the EX-OR 4T performed 4.02% and 4.27% better compared to the EX-OR 3T and EX-OR 6T respectively in terms of throughput. Finally, in terms of Energy Per Instruction, which is value of the product of toggle capacitance and its output voltage, the proposed EX-OR 4T saw an improvement of 13% and 15% respectively when compared with the EX-OR 3T and EX-OR 6T circuits.

In addition, the proposed 4 bit EX-OR circuits have shorter switching times. The charging time constant of series – parallel circuit is given in Eq. (1). The series-parallel circuit has a constant charging time, whereas the PFETs have been assumed to be of equal size in resistance and represents the capacitance between the upper and lower PFET groups.

$$\tau_p = R_p C_1 + 2R_p C_{out} \quad (1)$$

The time constant for the low-to-high transition is given in Eq. (4).

$$\tau_n = R_n C_2 + 2R_n C_{out} \quad (2)$$

Within the limits of this analysis, the two sides of transistor structure are symmetrical which results in a much simpler layout. The proposed circuit output is mainly dependent PGEN. There is an odd function when odd number of 1's gives and output equal to 1, with f = 0 otherwise. The proposed EX-OR 4T sharing connections are used between the output and the power supply (or) ground. The individual functions can be traced through each branch, while the circuit may appear somewhat complex at first sight. For example, the right NFET array directly implements the complement of the terms

$$a.b.c.d + a.b.c.d = a.(b.c + b.c).d = a.(b \oplus c).d \quad (3)$$

While the left array gives the complemented form of

$$a.b.c.d + a.b.c.d = a.(b \oplus c)d \quad (4)$$

Other terms of cross connections are generated in the same manner. The transient switching times are more complicated to deal with even though the construction of logic function via FET placement is straightforward. These functions are provided by Fig. 1 and its time constant related with the charging circuit is as follows:

$$\tau_p = C_{out}(R_{p1} + R_{p2} + R_{p3} + R_{p4} + R_{p5} + R_{p6}) \quad (5)$$

Similarly, the time constant associated with the discharging path is shown in Fig. 2.

$$\tau_p = C_{out}(R_{n1} + R_{n2} + R_{n3} + R_{n4} + R_{n5} + R_{n6}) \quad (6)$$

These above mentioned Eqs. (5) and (6) ignore parasitic capacitance that are associated with opposite polarity FETs. This yields switching delay in circuits. In this proposed circuit, the charging current will revolve around the response time of the single gate versus a conventional cascaded arrangement. According to the abovementioned analysis, the delays are measured and shown in Table 1. The simulated layouts areas are calculated using NMOS FET, PMOS FET aspect ratios. The total area is calculated via the number of transistor used in the circuit, input output pad and corresponding connection wires.

4.1. EX-OR based ECC circuit

The 4 input EX-OR based ECC circuit simulation results are shown in Table 2. The results show that the power dissipation of the circuit is 38nW for CMOS 70nm feature size. The designed EX-OR gates and other gates are properly arranged in a dynamic CMOS structure. There is no static power dissipation in the circuit due to push-pull configuration of the CMOS circuits. So, the circuit avoids critical path in every input and output patterns. The bit streams are applied to the circuits as logical '1' and logical '0' concept, which is fed to the modified ECC circuits. This proposed circuit sends a signal to the output node without any charge losses due to push-pull configuration and pass transistor configuration. The power dissipation, delay, area, latency and throughput have achieved their goals in our proposed circuit due to the abovementioned concept.

Table 2. Simulation results of 4-bit EX-OR 4T, 4-bit EX-OR 3T and 4-bit EX-OR 6T gate based ECC circuit.

Circuit	Size (nm)	Power $\times 10^{-09}$	Delay (ps)	Area (μm)	L (T) 10^{-09}	T Gbps	EPI(j/s) $\times 10^{-12}$
EXOR4T	70	38	83	1650	2.683	2.981	18.621
	90	75	222	1725	3.71	2.156	37.614
	120	13	247	2484	4.037	1.981	62.887
	180	24200	143	10619	3.036	2.635	186.02
EXOR3T	70	680	15	1335	0.557	0.143	18.847
	90	428	55.09	1380	0.894	8.941	39.508
	120	2950	56	8970	1.398	5.722	62.258
	180	4250	39	8970	1.33	6.015	186.02
EXOR6T	70	18660	20	1536	168.2	0.047	9.795
	90	46640	70	1600	0.905	0.088	7.159
	120	24990	0.08	2280	0.563	0.141	22.854
	180	231500	137	10209	2.4	3.334	90.820

The 4 bit EX-OR 4T circuit is compared with the 4 bit EX-OR 3T and 4 bit EX-OR 6T ECC circuit in terms of power dissipation, area, delay, throughput, latency and EPI for feature size 70nm and its corresponding voltage 0.7V. The EX-OR 4T has improved the improved the power dissipation by 94.4% and 99.7% as compared to the EX-OR 3T and EX-OR 6T respectively. This is probably due to the sub-threshold current that arises from the inversion charges which exist at the gate voltages below the threshold voltage. The EX-OR 4T as compared to the EX-OR 3T and EX-OR 6T ECC circuit has an improvement of 81% and 75% respectively in terms of delay due to the minimum average high-to-low propagation delay and low-to-high propagation delay. The maximum switching frequency f_{max} is always equal to $1/2t_p$, which allows the output transient of the inverter to be characterized by a RC charge/discharge model. Our proposed EX-OR 4T as compared to the EX-OR 3T and EX-OR 6T ECC circuit has improved our design by 19% and 6.9% in terms of area through advances in circuit design techniques and careful chip layout. The latency of our proposed EX-OR 4T as compared to the EX-OR 3T and EX-OR 6T ECC circuit has improved our design by 79% and 98% due to the impact of transistor parasitic capacitances, wiring capacitance, interconnect capacitance and input capacitance. The EX-OR 4T as compared to EX-OR 3T and EX-OR 6T ECC circuit has improved our circuit in terms of throughput by 95% and 98% respectively.

Similarly, the EX-OR 4T as compared to the EX-OR 3T and EX-OR 6T ECC circuit in terms of EPI has improved our circuit by 1.1% and 47% respectively.

The simulation results of the proposed 4 bit EX-OR 4T based ECC circuits are shown in Figs. 6, 7 and 8 respectively. The voltage versus time simulation results is shown Fig. 6 with a feature size of 70nm. The power dissipation is calculated using the output power and load power components. In normal operations, the N+ material body is tied to either ground or V_{DD} (if the transistor can be modelled as a three terminal device). The NMOS switch is turned off when the gate voltage is below some threshold V_t . The switch turns on forming a channel connecting source to drain when the gate voltage rises greater than V_t . When the transistor is in cut off region, I_{ds} is approximately zero. When the transistor is in linear mode, I_{ds} increases with V_{ds} . In saturation mode, I_{ds} is constant. The PMOS transistor is similar to NMOS transistor with reversed current flow direction and half of the current because of lower mobility.

The delay is calculated from its duty cycle of output waveform cycle and is shown in the graph (Fig. 6). The average current of the ECC operation and corresponding output voltage are indicated in Fig. 7. This graph gives identical values of output and input voltage.

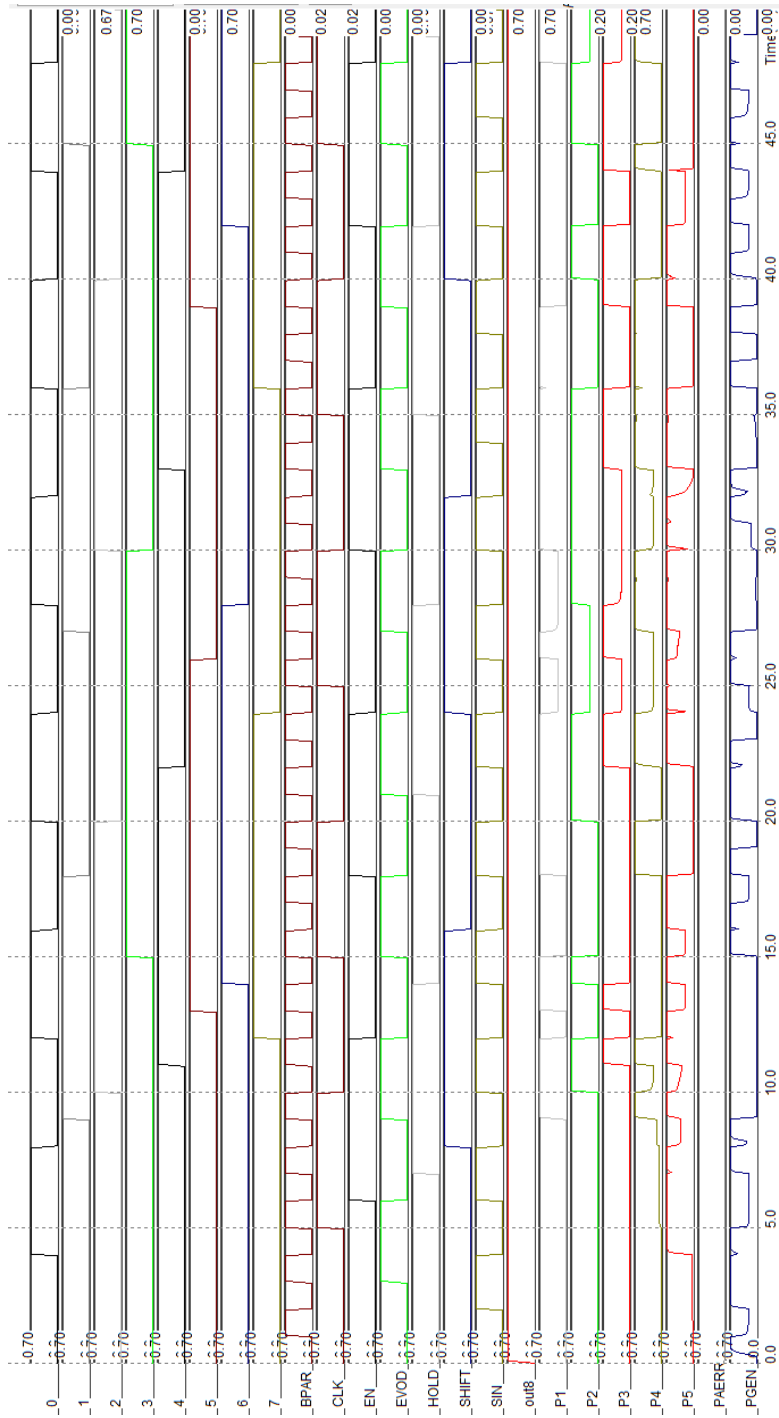


Fig. 6. ECC simulation results of voltage vs time for feature size 70nm.

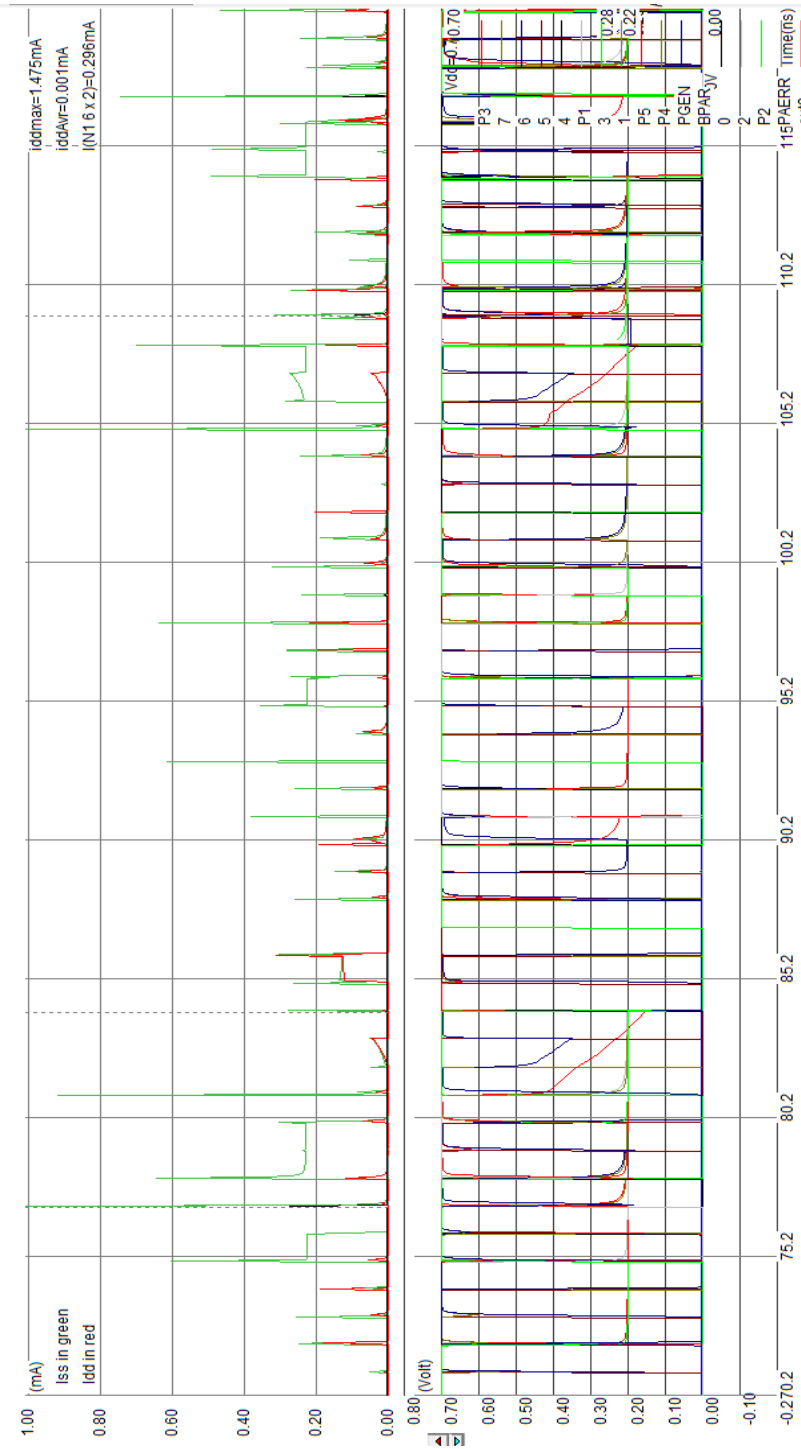


Fig. 7. ECC simulation results of voltage vs current feature size 70nm.

The ECC Voltage Transfer Characteristics (VTC) is shown in Fig. 8, which is qualitatively similar to that of the ideal inverter transfer characteristic. The output voltage V is equal to the high value of V_{OH} (output high voltage) because of the very low input voltage levels. In this case, the driver NMOS transistor is in interrupt, and hence, does not conduct any current. Accordingly, the output voltage level is high and the voltage drop across the load device is very small in magnitude. As the input voltage increases, the driver transistor starts conducting a certain drain current, and the output voltage eventually starts to decrease. Our proposed circuit has an ideal VTC characteristic which validates the design. The circuits are simulated using CMOS 70nm feature size and 0.7V for V_{DD} . According to Fig. 8 the V_{OH} is $\sim 0.69V$. According to VTC characteristic the V_{IH} should be $\frac{V_{DD}}{2}$ and our circuit gives exactly 0.35V. The V_{IL} is 0.001 and V_{OL} is

0. The worst case delay could be calculated using the noise margin formula:

$$N_{MH} = V_{OH} - V_{IH} = 0.69 - 0.35 = 0.34 \text{ and}$$

$$N_{ML} = V_{IL} - V_{OL} = 0.001 - 0.00 = 0.001$$

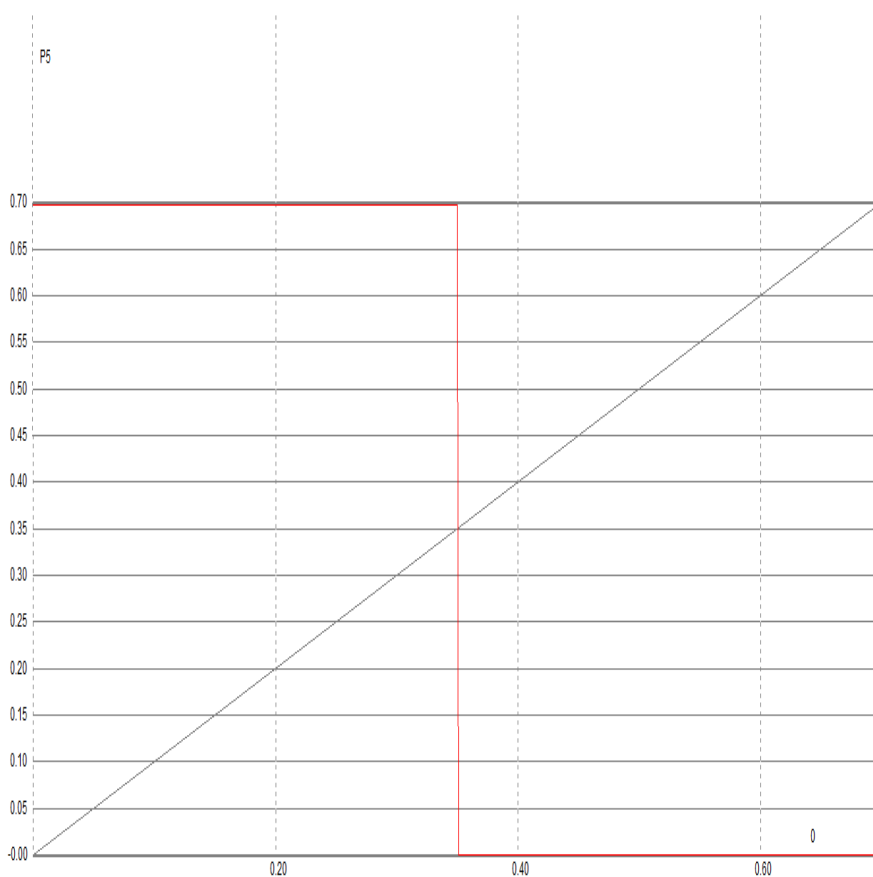


Fig. 8. VTC curve of ECC feature size 70 nm.

4.2. Parameter analysis of EX-OR 4T based ECC circuit and comparisons of the performance with hardening strategies.

4.2.1. Parameter analysis

The EX-OR 4T based ECC circuit is further analysed in terms of interconnect. The power dissipation of ECC circuits depends on parasitic capacitance, output voltage and its applying frequency. The parasitic capacitance is associated with source or drain of a transistor, which includes the gate-to diffusion overlap capacitance, C_{gol} , and the diffusion area and perimeter capacitance C_{jb} and C_{jbsw} . The whole EX-OR 4T based ECC circuit layout gives $1.699\mu\text{W}$ power dissipation which includes input/output pads. The ECC circuit threshold voltage are reported at 49mV for 70nm feature size using both a constant current. Threshold voltage hold normally decrease, but not as fast as channel length or supply voltage (because of sub threshold leakage). Hence, the output voltage is exactly given as input voltage due to push-pull configuration method.

The EX-OR 4T based ECC circuit saturation current has increased somewhat through aggressive device design as feature size decreases even though constant field scaling would suggest it should remain constant. The logic '0' input is on the order of few pico ampere per micron which can be exponentially increased because of subthreshold conduction through devices with low threshold voltage. The above three mentioned interconnect analysis parameter are shown in Fig. 9 which is analysed for feature size 70nm. The parametric analysis is calculated for the entire chip of the ECC circuit that covers the input pad, output pad, connecting wire and connecting nodes. The abovementioned components have highly leaking current which increases the total leakage current of the whole chip.

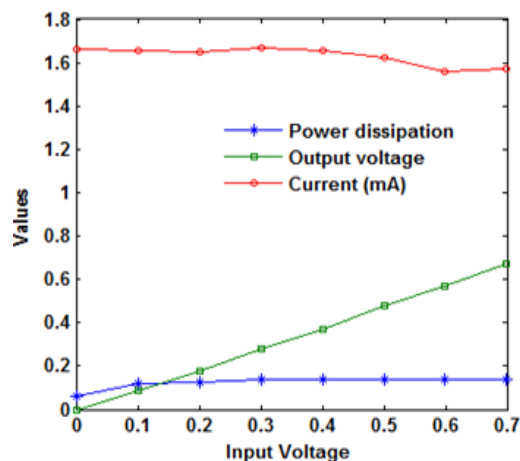


Fig. 9. Parameter analysis of ECC circuit.

4.2.2. Performance comparison with other hardening strategies

Our modified ECC circuits are compared with other existing circuits. Whatmaugh et al. [6] proposed an error correction circuit called the Razor method. This circuit occupies time borrow tracking logic and numerous memory circuits. The different combination of circuits deduce the energy and power according to their operation.

Therefore, it occupies more area as compared to our circuits. Kun Ma et al. [7] designed an ECC circuit using the LOEDAR method. Our circuit gives better performance than Kun Ma et al. [7] circuits in terms of delay and area due to less number of transistor used in the circuit and reduction in the critical path. Our modified ECC circuit reduced 97.59% power dissipation and 90.568% propagation delay than Sanguhn cha et al. [9] circuits. Sanguhn cha et al. [9] proposed H matrix circuit which is ODD weight column code which may give a complex operation in read and write data. Our modified ECC circuit give a regular manner of data and check of both parity bit by using Hamming code. Complexity is kept at a minimum in our modified circuit. The results in Table 3 clearly demonstrate the effectiveness of our method.

Table 3. Comparison table for modified ECC circuit performance with other strategy.

Circuit	Proposed	Ref. [6]	Ref. [7]	Ref. [8]	Ref. [9]
Power of reduction	38nW	---	---	1.58 μ W	391.9 μ W
Delay (ps) of reduction	83	---	60	880	---
Area (μm^2) of reduction	1650	185500	10636	19.5	---
Latency (ns) of reduction	2.683	99.91	84.48	-83.615	---
			---	----	0.55ns
			---	---	-84.5

5. Conclusion

This paper concisely explained the architecture of a proposed ECC circuit. The core component of the 4 input EX-OR is proposed and the subsidiary components are designed for the ECC circuit. The modified ECC circuit and its auxiliary components are schematized using DSCH and layouts are simulated using the Microwind CAD tools. The proposed EX-OR 4 transistor circuits would give enhanced execution results. The modified ECC circuit demonstrates low power dissipation (94.41%), and high throughput (95.20%) which gives better performance than existing circuits.

References

1. Ma, K.; and Wu, K. (2011). LOEDAR, A low cost error detection and recovery scheme for ECC. *Proceedings, Design, Automation & Test in Europe Conference & Exhibition (DATE)*, 2011,14-15 march 2011, pp 1-6.
2. Brewer, J.; and Gill, M. (2008). Nonvolatile memory technologies with emphasis on flash. A comprehensive guide to understanding and using flash memory devices. *IEEE Press Series on Microelectronics System, chapter 3, pp 63-123*.
3. Caramia, M.S.; Di Carlo, M.; Fabiano and Prinetto, P. Flare. (2009). A design environment for flash-based space applications. *Proceedings of High Level Design Validation and Test Workshop. HLDVT 2009. IEEE International*, 14-19.

4. Caramia, M.S.; Di Carlo, M.; Fabiano and Prinetto, P. (2009). Flash-memories in space applications: Trends and challenges. *Proceedings of East-West Design & Test Symposium (EWDTS)*, 18-21.
5. Agustin Dominguez-Oviedo.; and Anwar Hasan.M. (2009). Error detection and fault tolerance in ECSM using input randomization. *IEEE Transactions on dependable and secure computing*, 6(3), 175-187.
6. Caramia, M.; Fabiano M.; Miele, A.; Piazza, R; and Prinetto, P. (2010). Automated synthesis of edacs for flash memories with user-selectable correction capability. *Proceedings of IEEE International on High Level Design Validation and Test Workshop, HLDVT 2010*, , 113-120.
7. Stefano Di Carlo.; Michele Fabiano.; Roberto Piazza.; and Paolo Prinetto. (2010). EDACs and test integration strategies for NAND flash memories. *Design & Test Symposium (EWDTS), East-West*, 218-221.
8. Guo., X.; Fan, J.; Schaumont, P.; and Verbauwhede, I. (2009). Programmable and parallel ECC coprocessor architecture: Trade-offs between area, speed and security, *Cryptographic Hardware and Embedded System (CHES)*, 289-303.
9. Paul, N.; Whatmough, Shidhartha Das.; and David, M.Bull. (2014). A Low-power 1-GHz razor FIR accelerator with time-borrow tracking pipeline and approximate error correction in 65-nm CMOS, *IEEE Journal of Solid-State Circuits*, 49(1), 84-94.
10. Kun Ma.; and Kaijie Wu. (2014). Error detection and recovery for ECC: A new Approach against side-channel attacks. *IEEE Transactions on Computer-Aided Design of Integrated Circuits and Systems*, 33(4), 627-637.
11. Daniel G. T.; Matthieu A.; Fabrice S.; and Michel J. (2014). Soft error detection and correction technique for radiation hardening based on c-element and BICS. *IEEE Transactions on Circuits and Systems-II: Express Briefs*, 61(12), 952-956.
12. Sanguhn Cha.; and Hongil Yoon. (2012). Efficient implementation of single error correction and double error detection code with check bit pre computation for Memories. *Journal of Semiconductor Technology and Science*, 12(4), 418-425.
13. Rajkumar, R.; Ramkumar, N.; and Vignesh, M. (2014). An area efficient error correction codes to protect against stuck-at defects and soft errors. *International Conference on Communication and Signal Processing, India, Melmaruvathur, 2014*, pp. 066-070.
14. Neil, H.E.; and Weste David Harris Ayan Banerjee. CMOS VLSI Design. (Third edition). A Circuits and Systems Perspective.
15. Zarandi, H.R.; Miremadi, S.G.; and A. Ejlali. (2003). Dependability analysis using a fault injection tool based on synthesizability of HDL models, *Proc. 18th IEEE International Symposium Defect Fault Toler. VLSI System*, pp: 485-492.
16. Chari, S.N. (2010). Designing a side channel resistant random number generator. *Proceedings of the 9th International Federation for Information Processing WG 8.8/11.2 International. Conference. SmartCard Research. Advanced.Application*, 49-64.